

See discussions, stats, and author profiles for this publication at: <https://www.researchgate.net/publication/373012303>

On Applications of TiO₂ Quantum Dots to Solution of Optogenetics Problems

Article · May 2023

DOI: 10.33581/1561-4085-2023-26-1-98-105

CITATIONS

0

READS

57

6 authors, including:



[Olga M. Fedotova](#)

Russian State Social University

71 PUBLICATIONS 123 CITATIONS

[SEE PROFILE](#)



[Oleg Khasanov](#)

National Academy of Sciences of Belarus

110 PUBLICATIONS 126 CITATIONS

[SEE PROFILE](#)



[Grigory Rusetsky](#)

National Academy of Sciences of Belarus

39 PUBLICATIONS 29 CITATIONS

[SEE PROFILE](#)

On applications of TiO₂ quantum dots to solution of optogenetics problems

O. Khasanov,* R. Rusetsky, O. Fedotova, and D. Klezovich
*Scientific and Practical Materials Research Center,
National Academy of Sciences of Belarus,
P. Brouki str. 19, 220072, Minsk, Belarus*

A. Pashkevich
*Institute for Nuclear Problems of Belarusian State University,
Babruiskaya str. 11, 220030 Minsk, Belarus*

K. Pistsova and Ya. Gorbach
*Physics Faculty, Belarusian State University,
Niezaliežnasci ave 4, 220030 Minsk, Belarus*

D. Zharkov
*Zavoisky Physical-Technical Institute KSC RAS,
Sibirsky tract 10/7, 420029, Kazan, Russia
(Dated: January 13, 2023)*

Features of echo signals in titanium dioxide quantum dots (QD) excited by two femtosecond noncollinear laser pulses are under consideration. It is shown that in addition to well-known primary photon echo, under appropriate phase-matching conditions at resonant frequency, echo responses at multiple frequencies due to the large permanent dipole moment are generated but at different phase-matching conditions. This provides high degree of excitation and characterization of investigated objects at necessary frequency. In other words, we predict parametric generation of echo signals at upconversion frequencies by the IR laser pulses in the TiO₂ QDs. Accounting for nontoxicity of these QDs for living cells we suppose that such particles can ensure the delivery of light of necessary spectral content to local areas of the human body. All this will pave the way for the use of up-conversion echoes in TiO₂ QDs for optogenetics.

PACS numbers: 42.65.Ky; 42.65.-k; 71.20.Nr; 87.64.-t

I. INTRODUCTION

The idea of cells control by light was born long ago, but its implementation became possible only at the beginning of the 21st century due to the scientific and technologic developments, and primarily genetic engineering. Currently, optogenetics as a method of neuromodulation, based on combination of optical and genetic methods to control the activity of individual neurons in living tissues, is actively developing. The method of optogenetics provides new opportunities for studying the structure and functions of the brain and is more subtle and accurate than the widely used methods of electrical stimulation. It has great prospects to heal Alzheimer's, Parkinson's and other brain diseases, to combat neoplasma, to suppress chronic pain and depression, to develop optogenetic brain implants and so on. Optogenetics methods will find application in neurology, cardiology, ophthalmology, and in the treatment of muscle dysfunctions. Finally, the ideas of optogenetics will be useful for creating supercomputers based on artificial intelligence, the Neuronet, etc.

The essence of the optogenetics is that only the necessary neurons or nerve tissues begin to react to light due to genetic modification. With the help of modern optical techniques, the light changing the behavior of nerve cells can be painlessly and precisely delivered to the target in vivo. While there are different approaches to do it, there is a great need to develop non-invasive methods for delivering visible radiation to photosensitive receptors. At the same time, living tissues that are transparent to near-IR radiation absorb visible light. Therefore, an obvious this problem solution to can be the use of nanoparticles providing upconversion of near-IR radiation into visible light. Such nanoparticles must be biocompatible and highly efficient for the spectral conversion of light. Modern technologies allow to fabricate nanoparticles with inherent properties useful for non-invasive visualization, characterization and control of biological processes at cell and molecular level that provides correct diagnostics and treat diseases [1–3]. Moreover, such particles will ensure the delivery of drugs to local areas of the human body. What's more, these capabilities can be combined for simultaneous in vivo diagnosis, delivery path tracking, and real-time treatment.

* olkhas65@gmail.com; Scientific and Practical Materials Research Center, National Academy of Sciences of Belarus, P. Brouki str. 19, 220072, Minsk, Belarus

II. NANOMATERIALS FOR OPTOGENETICS

Among the large variety of nanomaterials prospective for biomedical applications nanoparticles with rare earth (RE) dopants draw scientific attention due to their unique properties to absorb near IR-radiation and emit light in visible and UV spectral range [4]. It is especially important for medicine, because the living cells are transparent for IR photons. Thus, this opens the door for deep penetration of light into biotissues [5] and development of multifunctional nanoprobes. Upconversion nanoparticles underlying theranostics could enable simultaneous diagnosis and treatment of diseases [6]. It should be noted, upconversion particles with rare earth elements are biocompatible with living cells [7]. Due to the presence of several metastable states, as well as the relatively slow nonradiative relaxation of intermediate electronic levels, various upconversion schemes in the system of energy levels of RE ions are highly efficient. Presently upconversion luminescence properties of nanocrystals doped with RE ions enabling their application to optogenetics are under active study. From this point of view, as shown, fluoride matrices have a good chance of being used due to their thermal, optical, and chemical stability, as well as low nonradiative losses. Among fluorides hexagonal β - NaYF_4 nanocrystals are considered the most efficient matrices for upconversion ions Er and Yb [8]. Luminescence quantum yield of nanocrystal can be amplified through core-shell or core-shell-shell structure formation. In comparison with fluorides matrices from yttrium orthovanadate have good crystal structure quality, are thermally stable and also reactive. Despite the fact that luminescence is mainly determined by the nature of the rare-earth ion, the matrix with incorporated ions affects the position of the peaks of the luminescent lines through its crystalline field. The intensity of luminescence depends on the method and temperature regime of synthesis, the composition of the base matrix, the size and shape of nanoparticles, and also on the concentration of the rare earth ions. Excitation of upconversion luminescence can be effective if several criteria are met: ions have metastable levels and the so-called ladder structure of levels. Another criterion that upconversion materials must satisfy is a low multiphonon relaxation rate, since a high relaxation rate significantly reduces the lifetime of excited states. The concentration of rare-earth elements in crystals should be optimal, since at a low concentration the luminescence intensity is low, and at a high concentration, the cross-relaxation rate increases, which leads to nonradiative transitions from excited levels. YVO_4 nanocrystals doped with Yb^{3+} and Er^{3+} satisfy the above criteria. Fig.1 shows the system of levels of Yb^{3+} and Er^{3+} ions, which demonstrates the schemes of energy transfer from a donor to an acceptor.

Presented at Fig.1 scheme of upconversion luminescence is a main mechanism of energy transfer from donor to acceptor. Two-quantum excitation through an intermediate level and cross-relaxation can give an additional

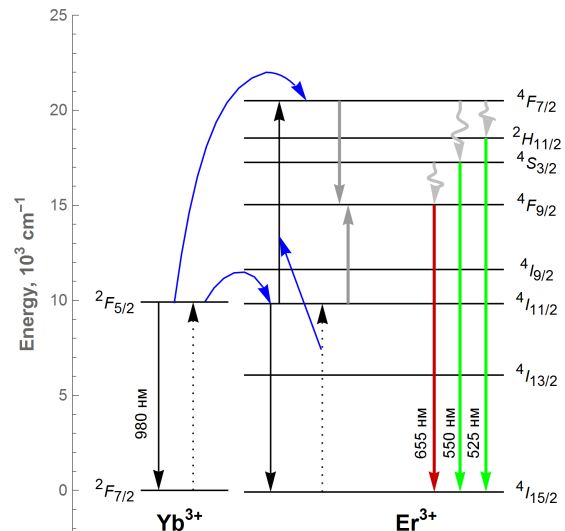


FIG. 1. Scheme of energy transfer from the Yb^{3+} donor ion to the Er^{3+} acceptor ion.

contribution to the luminescence. The efficiency of these upconversion mechanisms in Er^{3+} ions is high due to the close energy difference between some energy levels

III. FEATURES OF TiO_2 QUANTUM DOTS

Semiconductor quantum dots (QDs) attract attention of scientists due to their unique properties. The adjustable optical properties of QDs open the doors for their applications in different areas such as: biomedical applications, lasing, harmonic generation, detection and emission of THz radiation, security systems, wireless communication systems, UV protection system, superior strength fibers and films and so on. As is shown in [9] TiO_2 QDs incorporated into potassium dihydrogen phosphate crystals provide enhancement of the second harmonic generation efficiency at higher than 60 % in comparison with pure KH_2PO_4 . Moreover, according to [10] this material has large Kerr nonlinearity. A remarkable feature of almost all semiconductor QDs including TiO_2 QDs is the presence of a permanent dipole moment (PDM). According to estimations [11] the PDM magnitude of the CdSe QD exceeds hundreds Debye. In [12] the authors have revealed in the experiment the very large PDM of excitons of InAs QDs in GaAs, corresponding to electron-hole separations up to 2.5 nm. ZnO QD has the advantage of having the PDM 11.4 times and 5,21 times larger than those of CdSe and CdS, respectively [13, 14]. A large value of the PDM is also inherent in the TiO_2 QDs [15]. It is evident that large value of the PDM impacts on the QD properties. The rich structure of exciton levels due to the strong electron-hole interaction is predicted to be formed with a multiple of possible permitted transitions Fig.2 [16, 17]. Below we discuss the upconversion properties of photon echo signals (PE) in

TiO₂ QDs and their potential for solution of optogenetics problems accounting for their non toxicity for living cells.

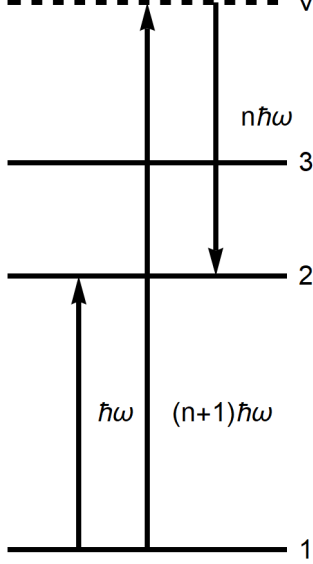


FIG. 2. Scheme of single- and double-quantum transitions in quantum dot

IV. MODEL

So, let us dwell on the task of femtosecond laser pulse interaction with the three-level QDs incorporated into transparent dielectric matrix with quadratic nonlinearity. We suppose that the light pulse

$$E_L = E_1(r, t) \cos(\omega_1 t - kz + \varphi_1(z, t)) \quad (1)$$

with an amplitude $A(r, t)$, carrier frequency ω , wave vector k and phase $\phi(z, t)$ is in resonance with the lowest transition in QD (see Fig.1). With considering the PDM the QD Hamiltonian is following:

$$\hat{H} = \begin{pmatrix} \hbar\Omega_1 - p_{11}E_L & -p_{12}E_L & -p_{1n}E_L \\ -p_{12}E_L & \hbar\Omega_2 - p_{22}E_L & -p_{2n}E_L \\ -p_{n1}E_L & -p_{n2}E_L & \hbar\Omega_n \end{pmatrix} \quad (2)$$

Here $\hbar\Omega_i$ is the energy of i -th level, p_{ij} is the dipole moment of ij transition, $(p_{11} - p_{22})$ is the PDM.

Owing to the unitary transformation

$$\hat{L}_1 = \begin{pmatrix} \exp(i\lambda) & 0 & 0 \\ 0 & \exp(-i\lambda) & 0 \\ 0 & 0 & 1 \end{pmatrix}, \quad (3)$$

where

$$\lambda = \frac{p_{11}}{\hbar} \int E_1 dt = \sum_{m=1}^{\infty} \frac{\vec{p}_{11} \vec{E}_1}{\hbar\omega} \sin \varphi(z, t), \quad (4)$$

$\varphi(z, t) = (\omega t - kz)$, we arrive at Hamiltonian describing QD interaction with a set of fields at multiple frequencies [20]

$$\hat{H}' = \begin{pmatrix} \hbar\Omega_1 & -p_{12} \sum_{m,s} \bar{E}_{m,s}^L e^{i\varphi_{m,-s}} & -p_{1n} \sum_{m,s} E_{m,s}^L e^{i\varphi_{m,-s}} \\ -p_{21} \sum_{m,s} \bar{E}_{m,s}^L e^{i\varphi_{m,s}} & \hbar\Omega_2 & -p_{2n} \sum_{m,s} E_{m,s}^L e^{i\varphi_{m,s}} \\ -p_{n1} \sum_{m,s} E_{m,s}^L e^{i\varphi_{m,s}} & -p_{n2} \sum_{m,s} E_{m,s}^L e^{i\varphi_{m,s}} & \hbar\Omega_n \end{pmatrix} \quad (5)$$

In other words, the interaction of QD owing the PDM with the laser pulse is equivalent to its interaction with a multifrequency field. These fields can induce one- and two-photon transitions between levels $|1\rangle$ and $|2\rangle$. Here $E_{ms}^L = E_m^L J_s(a)$, $\bar{E}_{ms}^L = E_m^L J_s(2a)$, $\phi_{m,\pm s} = \phi_m \pm s\phi_1$, $a = p_{11} \cos \alpha E_1 / \hbar\omega_1$, $J_s(a)$ is the Bessel function of s -th order. Restricting ourselves to the consideration of the resonances of the first and second orders by following transformation [21].

$$\hat{L}_2 = \exp(-iS) = 1 - iS - \frac{1}{2}SS + \dots \quad (6)$$

we obtain Hamiltonian for a generalized two-level system

$$\hat{H}'' = \begin{pmatrix} H''_{11} & H''_{12} \\ H''_{21} & H''_{22} \end{pmatrix}, \quad (7)$$

where nondiagonal element

$$H''_{12} = -p_{12} \sum_m \bar{E}_{m,m-1} e^{i\varphi_1 + \theta_m} - \frac{p_{1n} p_{n2}}{2\hbar}.$$

$$\cdot \sum_{m,s,k,p} E_{ms} E_{kp} \frac{\Omega_{n1} - \dot{\varphi}_{m,-s} + \Omega_{n2} - \dot{\varphi}_{k,p}}{(\Omega_{n1} - \dot{\varphi}_{m,-s})(\Omega_{n2} - \dot{\varphi}_{k,p})} e^{i(\varphi_{m,-s} - \varphi_{k,p})} \quad (8)$$

describes single- (first term) and double-quantum (second term) transitions between resonant levels and in diagonal elements.

$$H'_{11} = W_1 + \Delta W_1 \text{ and } H'_{22} = W_2 + \Delta W_2, \quad (9)$$

ΔW_i include Stark shifts of levels. After unitary transformation

$$\hat{L}_3 = \begin{pmatrix} \exp(-\frac{i}{2}\varphi_1) & 0 \\ 0 & \exp(\frac{i}{2}\varphi_1) \end{pmatrix} \quad (10)$$

we arrive at the Hamiltonian for the generalized two-level system in rotating reference framework. In this case, the Hamiltonian does not contain rapidly oscillating terms, and the dynamics of spectroscopic transitions obeys the following vector model:

$$\dot{\vec{R}} = [\vec{\Omega} \times \vec{R}], \quad (11)$$

where $R_1 = \rho_{12} + \rho_{21}$, $R_2 = i(\rho_{12} - \rho_{21})$, $R_3 = \rho_{11} - \rho_{22}$, $\Omega_1 = \frac{1}{\hbar}(H'_{12} + H'_{21})$, $\Omega_2 = \frac{i}{\hbar}(H'_{12} - H'_{21})$, $\Omega_3 = \frac{1}{\hbar}(H'_{11} - H'_{22})$, R_i is the i -th component of Bloch vector.

From (11) it is easy to deduce the Bloch equation system for the QD polarization component and population difference in the slowly varying envelope approximation:

$$\dot{R}_- = i(\delta + \delta_s - \delta_L^{ef} R_3)R_- - 2iE_{ief}R_3, \quad (12)$$

$$\dot{R}_3 = i(E_{ief}R_+ - E_{ief}^*R_-) \quad (13)$$

Bloch equation system is presented in dimensionless form, where $R_- = R_1 - iR_2$;

$E_{ief} = (p_{12}\bar{E}_i/\hbar\omega_p)(J_0(2a_i) + J_2(2a_i))$, $i = 1, 2$;
 $\delta = \Delta/\omega_p$; $t = \omega_p T$; $\omega_p^2 = 2\pi N d_{12}\omega_1/\hbar n_1^2$;

ω_p is plasma frequency;

δ is carrier frequency detuning from resonance;

δ_s is Stark shift of level $\delta_s = (\Delta W_2 - \Delta W_1)/\hbar$;

$\Delta W_i = \eta_{im}E_m^2$;

$\eta_{im} = \sum_{n \neq 1,2} (p_{in}p_{ni}/\hbar)(2\Omega_{ni}/(\Omega_{ni}^2 - \omega_m^2))$;

δ_L^{ef} is excitation induced shift due to dipole-dipole interaction [16].

In equation (12) for induced dipole moment, the first term describes detuning from resonances including dynamic frequency shift due to quadratic Stark effect and local field impact. The second term accounts for one- and two-photon absorption. Standard approach to solution of the Eq. set (12),(13) by use of Laplace transformation with corresponding initial conditions defined by preliminary excitation and by its decay, as well as some other methods of calculation of resonant medium responses [22], allow us to compute the photoinduced macroscopic polarization, which is source of the spontaneous responses. So, it easy to see, that macroscopic polarization induced by the first pulse contains multiple harmonics originated from the PDM contribution (we'll omit the Bessel function argument for brevity):

$$P(\tau_{pl}) = \sum_{m=1} \{(\alpha_m + \Delta\alpha_m R_3)E_m \cos \varphi + [p_{12}J_{m-1} + \frac{\kappa_{12}^{(m)}}{2}E_1 J_m]R_- e^{i\varphi_m}\} + c.c. \quad (14)$$

Without repeating the well-known method of solving the Bloch equations at the time of the first pulse and within the time interval between the first and second pulses we give the initial conditions for the equations in the reference framework associated with the second pulse:

$$R_1(t - \tau_{p1} - \tau_{12}) = R_1(\tau_{p1}) \cos[m(\vec{k}_2 - \vec{k}_1)\vec{r}' - \Delta\tau_{12}] + R_2(\tau_{p1}) \sin[m(\vec{k}_2 - \vec{k}_1)\vec{r}' - \Delta\tau_{12}]$$

$$R_2(t - \tau_{p1} - \tau_{12}) = R_1(\tau_{p1}) \sin[m(\vec{k}_2 - \vec{k}_1)\vec{r}' - \Delta\tau_{12}] - R_2(\tau_{p1}) \cos[m(\vec{k}_2 - \vec{k}_1)\vec{r}' - \Delta\tau_{12}]$$

where $m = 0, \pm 1, \pm 2, \dots$. It is evident, that the second pulse interaction with the macroscopic polarization results in recording polarization grating in the nanocomposite at multiple frequencies. Therefore one can expect, that echo signals due to the diffraction of polarization in-

duced by the second pulse at this grating will be emitted at different directions and at different frequencies.

V. PHOTON ECHO SIGNALS IN QUANTUM DOT ENSEMBLE WITH PERMANENT DIPOLE MOMENT

Solving the Eqs. (12 -13) for the moment of the second pulse action and after it, we have calculated the macroscopic polarization and photon echo (PE) signals in nanocomposite. As is known the emission frequency of QDs depends on their sizes, which leads to inhomogeneous broadening the nanocomposite spectral line because of spatial dispersion of the QDs. Moreover, we need to account for spatial dispersion of dipole moments and the QD spatial dispersion and distribution function of the dipole moment orientation within QDs relative to field polarization. In view of the above, under two-pulsed noncollinear excitation and a weak local field effect, viz. excitation induced shift, the macroscopic polarization is

the following:

$$P(t) = \sum_{m=1, n=0} e^{-i\varphi_n} \iiint P_m(\Delta, \Delta r, \alpha) g(\Delta) d\Delta \quad (15)$$

Here:

$$\varphi_n(z, t) = n(\omega t - \vec{k} \vec{r}),$$

$$P_m(\Delta, \Delta r, \alpha) = (p_{12} J_{m-1} + (1/2) \kappa_{12}^{(m)} E J_{m-2}) R_+,$$

$$R_+ = F(\theta_1, \theta_2) e^{im(\vec{k}_2 - \vec{k}_1) \vec{r}} e^{-i\Delta(t - 2\tau_{12})},$$

$$F(\theta_1, \theta_2) = \sin(\theta_1) \sin^2(\theta_2/2),$$

for the case of ultrashort excitation pulses. In difference from classical primary photon echo, the areas of excitation pulses rely on δ_s : $\theta_i = \tau_{pi} \sqrt{4E_{ief}^2 + \delta_s^2}$, $\delta = \omega_{12} - \omega_i$.

We suppose that inhomogeneous spectral line is described by Gaussian function. According to the literature data, the most pertinent distribution the QD radii is also Gaussian function. Averaging the induced polarization on inhomogeneous broadening displays, that all echo signals emitted at the same time moment $t \approx \tau_{12}$. Let us dwell on phase-matching conditions for multiple echo harmonics. The case $m = 1$ and $n = 1$ corresponds to the primary photon echo generation at resonant frequency ω_1 in $(2\vec{k}_2 - \vec{k}_1)$ direction under diffraction of the polarization wave on dynamic grating. For $m = 1$ and $n = 2$ one observes the echo signal at double frequency in $(3\vec{k}_2 - \vec{k}_1)$ direction. The cases $n = 3$ and $n = 0$ for $m = 1$ correspond to echo-responses at triple and terahertz frequencies, correspondingly. The scheme of the photon echo excitation and the phase-matching conditions for echo-signals are represented (for $m = 1, 2, n = 0, 1, 2, 3$) in the Fig.3. Length of the vectors correspond to the relative intensities of the echo-harmonics. The conditions $m \neq 1$ and $n = 1$ describe echo-signals at resonant frequency, emitted in $(m+1)\vec{k}_2 - m\vec{k}_1$ directions. Note that the responses at double and terahertz frequencies are proportional to p_{11} , while signal at triple frequency is proportional to p_{11}^2 .

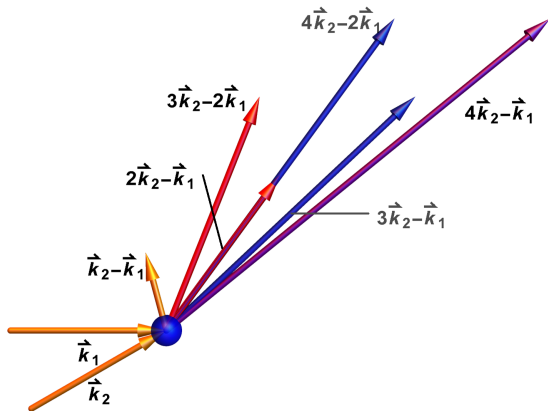


FIG. 3. Directions of echo signal generated in media with PDM

VI. CONCLUSIONS

Thus, photon echo features in titanium dioxide quantum dots (QDs) are studied. Spectral composition, observation time and phase-matching conditions for echo-responses excited by two noncollinear pulses are analysed. More specifically, the spectral and spatial features of echo signals due to the FDM inherent in quantum dots, as well as the effect of the spatial dispersion of transition dipole moments, are revealed. To the best of our knowledge, the effect of the PDM being of large value in semiconductor QDs on echo signals is first studied in detail. Oscillations of the PDM in laser pulse field are shown to be similar to action of multi frequency pulse, which can induce multiphoton transitions between resonant levels. We restrict ourselves to considering more intensive one- and two- quantum transitions. It has been revealed, that PDM is responsible for signals generated at multiple frequencies. Moreover, the responses at double and terahertz frequencies are proportional to magnitude of the PDM, echo signal at triple frequency is proportional to the square of this quantity and amplitude of n -th echo harmonics is proportional to . All echo-responses are emitted practically at the same time. According to obtained results, spatial dispersion of dipole moments in nanocomposites influences only on even responses. Summarizing the above, we predict parametric generation of echo signals at upconversion frequencies by the IR laser pulses in the TiO₂ QDs. Accounting for nontoxicity of these QDs for living cells we suppose that such particles can ensure the delivery of light of necessary spectral content to local areas of the human body. All this will pave the way for the use of up-conversion echoes in TiO₂ QDs for optogenetics

VII. ACKNOWLEDGEMENT

This work was supported by the project Φ 21PM-119 (A.P., D.K., K.P.) under the The Belarusian Republican Foundation for Fundamental Research (BRFFR)

-
- [1] L. Yan, F. Zhao, S. Li, Z. Hu, and Y. Zhao, Low-toxic and safe nanomaterials by surface-chemical design, carbon nanotubes, fullerenes, metallofullerenes, and graphenes, *Nanoscale* **3**, 362 (2011).
- [2] Q. Xiao, W. Bu, Q. Ren, S. Zhang, H. Xing, F. Chen, M. Li, X. Zheng, Y. Hua, L. Zhou, W. Peng, H. Qu, Z. Wang, K. Zhao, and J. Shi, Radiopaque fluorescence-transparent TaOx decorated upconversion nanophosphors for in vivo CT/MR/UCL trimodal imaging, *Biomaterials* **33**, 7530 (2012).
- [3] L. Cheng, C. Wang, and Z. Liu, Upconversion nanoparticles and their composite nanostructures for biomedical imaging and cancer therapy, *Nanoscale* **5**, 23 (2013).
- [4] M. Lin, Y. Zhao, S. Wang, M. Liu, Z. Duan, Y. Chen, F. Li, F. Xu, and T. Lu, Recent advances in synthesis and surface modification of lanthanide-doped upconversion nanoparticles for biomedical applications, *Biotechnology Advances* **30**, 1551 (2012).
- [5] L.-L. Li, R. Zhang, L. Yin, K. Zheng, W. Qin, P. R. Selvin, and Y. Lu, Biomimetic surface engineering of lanthanide-doped upconversion nanoparticles as versatile bioprobes, *Angewandte Chemie International Edition* **51**, 6121 (2012).
- [6] N. M. Idris, M. K. Gnanasammandhan, J. Zhang, P. C. Ho, R. Mahendran, and Y. Zhang, In vivo photodynamic therapy using upconversion nanoparticles as remote-controlled nanotransducers, *Nature Medicine* **18**, 1580 (2012).
- [7] A. Gnach, T. Lipinski, A. Bednarkiewicz, J. Rybka, and J. A. Capobianco, Upconverting nanoparticles: assessing the toxicity, *Chemical Society Reviews* **44**, 1561 (2015).
- [8] X. Teng, Y. Zhu, W. Wei, S. Wang, J. Huang, R. Nacache, W. Hu, A. I. Y. Tok, Y. Han, Q. Zhang, Q. Fan, W. Huang, J. A. Capobianco, and L. Huang, Lanthanide-doped $\text{Na}_x\text{ScF}_{3+x}$ nanocrystals: Crystal structure evolution and multicolor tuning, *Journal of the American Chemical Society* **134**, 8340 (2012).
- [9] V. Y. Gayvoronsky, M. A. Kopylovsky, M. S. Brodyn, I. M. Pritula, M. I. Kolybaeva, and V. M. Puzikov, Impact of incorporated anatase nanoparticles on the second harmonic generation in KDP single crystals, *Laser Physics Letters* **10**, 035401 (2013).
- [10] R. Adair, L. L. Chase, and S. A. Payne, Nonlinear refractive index of optical crystals, *Physical Review B* **39**, 3337 (1989).
- [11] F. P. Phony-Baloney, *Fighting Fire with Fire: Festooning French Phrases*, PhD dissertation, Fanstord University, Department of French (1988), a full PHDTHESIS entry.
- [12] A. Högele, S. Seidl, M. Kroner, K. Karrai, R. J. Warburton, M. Atatüre, J. Dreiser, A. Imamoğlu, B. D. Gerardot, and P. M. Petroff, Voltage-controlled electron-hole interaction in a single quantum dot, *Journal of Superconductivity* **18**, 245 (2005).
- [13] M. Shim and P. Guyot-Sionnest, Permanent dipole moment and charges in colloidal semiconductor quantum dots, *The Journal of Chemical Physics* **111**, 6955 (1999).
- [14] L. shi Li and A. P. Alivisatos, Origin and scaling of the permanent dipole moment in CdSe nanorods, *Physical Review Letters* **90**, 10.1103/physrevlett.90.097402 (2003).
- [15] P. Kania, M. Hermanns, S. Brünken, H. Müller, and T. Giesen, Millimeter-wave spectroscopy of titanium dioxide, TiO₂, *Journal of Molecular Spectroscopy* **268**, 173 (2011).
- [16] S. I. Pokutnii, Exciton states formed by spatially separated electron and hole in semiconductor quantum dots, *Technical Physics* **60**, 1615 (2015).
- [17] P. Klenovský, J. Valdhans, L. Krejčí, M. Valtr, P. Klapetek, and O. Fedotova, Interplay between multipole expansion of exchange interaction and coulomb correlation of exciton in colloidal II–VI quantum dots, *Electronic Structure* **4**, 015006 (2022).